

# Synthesis of polyanthranilic acid–Au nanocomposites by emulsion polymerization: development of dopamine sensor

BHAVANA GUPTA<sup>\*†</sup>, AMBROSE MELVIN<sup>1</sup> and RAJIV PRAKASH

School of Materials Science and Technology, Indian Institute of Technology, Banaras Hindu University, Varanasi 221 005, India

<sup>1</sup>Department of Chemistry, University of Pune, Ganeshkhind, Pune 411 007, India

<sup>†</sup>Present address: Surface and Nanoscience Division, Materials Science Group, Indira Gandhi Centre of Atomic Research, Kalpakkam 603 102, India

MS received 16 April 2013; revised 14 October 2013

**Abstract.** Polyanthranilic acid (PANA) and polyanthranilic acid–gold (PANA–Au) nanocomposites have been synthesized through emulsion polymerization technique. Use of gold chloride as an oxidant for anthranilic acid not only provides a new route for chemical synthesis of PANA, but also explores a facile method for the formation of nanocomposites. Emulsion polymerization helps in slowing down kinetics of polymerization in comparison to one-phase polymerization and thereby induces formation of monodispersed, both pure and Au nanoparticles, embedded PANA sphere. Reaction progress of nanocomposite formation is studied by UV–Vis spectroscopy for 0–24 h. PANA–Au nanocomposites are characterized by SEM, equipped with EDS, TGA, FT–IR, XRD and electrochemical techniques. XRD of nanocomposites depicts the amorphous nature of polymer and crystalline nature of Au with crystallite size of ~24 nm. Differential pulse voltammetry has shown the electro-active nature of PANA. The nanocomposites with improved thermal properties show good dispersion in common organic solvents, and it can be explored for application in interference-free dopamine sensors with sensitivity 12.5  $\mu\text{A}/\text{mM}$ . Acidic group (–COOH) on the polymer makes the sensor free from ascorbic acid interference.

**Keywords.** Polyanthranilic acid; nanocomposite; *in situ* polymerization; emulsion polymerization; nanoparticles.

## 1. Introduction

Conducting polymer is one of the most applicable materials either in pristine or in modified form, as it exhibit various desirable and switchable electrical, optical and magnetic properties. The proposed applications of conducting polymers are nanoscale electronics (Singh *et al* 2008; Jin *et al* 2009; Singh *et al* 2010), photonics (Nielsen *et al* 2005), sensors (Banik *et al* 2008; Mohan and Prakash 2010), and energy storage (Gupta and Prakash 2009). In addition, composite formation is an easiest approach to increase applicability of conducting polymers to a broader range of devices. Among the composite, nanocomposite have recently garnered significant attention because of their unique and synergistic physiochemical property (Mirkin and Letsinger *et al* 1996; Boal *et al* 2000; Maheshwari and Saraf *et al* 2006). Nanocomposites are not only known for their nano-dimension but also for exhibiting synergistic properties due to the combination of its two different components, i.e. matrix and filler, in particular, conducting polymer and metal-based nanocomposites

formed by decorating a conducting polymer with metal nanoparticles such as Ag, Au, Pt or Pd (Hable and Wrigton 1991; Majumdar *et al* 2005, 2006; Tseng *et al* 2005) have been reported for multiple technological application related to catalysis, sensors, electronic devices like transistor, etc. In general, there are two suitable methods of synthesis of conducting polymer metal-based nanocomposite. In the first method, nanoparticle separately synthesized followed by polymerization around the particles or dispersion of the nanoparticle in a polymer matrix (Dewald *et al* 2005; Mallick *et al* 2009; Melvin *et al* 2010), whereas in the second method, both polymerization and reduction of metal ion to nanoparticle takes place simultaneously (Mallick *et al* 2006; Selvaraj and Alagar 2008; Power *et al* 2010). Most of the reports related to conducting polymer nanocomposites are dealt with PANI–Au and other nonprocessable polymer. In this cases, the evidence of functionalization or co-ordinative interaction between metal and polymer have neither been mentioned nor discussed. Thus, it is required to select a polymer as well as a synthetic approach by which a complexation takes place between the metal and the polymer and that will become more useful for further application.

\*Author for correspondence (bgupta1206@gmail.com)

Nanoparticle-incorporated conducting polymeric matrices are of recent technological interest in the development of sensor. Amongst various kinds of nanocomposites, special attention has been given to conducting polymers-Au based nanocomposite due its capability in detecting different types of analyte. Dopamine (DA) which is indeed one of the crucial analyte present in extra-cellular fluid of mammalian central nervous system (CNS) with low and varying basal concentration (nano to micromolar range) (Downard *et al* 1995) shows the difficulty in the voltammetric detection due to ascorbic acid (AA) interference. Conducting polymer-Au matrix is already reported for DA estimation by voltammetric technique. It describes that conducting polymer are responsible for both selective and catalytic oxidation of DA and uric acid. While the enhancement in sensitivity up to nanomolar level occurred due to the presence of Au particles (Mathiyarasu *et al* 2008). Some conducting polymers have been used for dopamine sensor without AA interference (Tu *et al* 2007; Pandey *et al* 2009). However, there is no report related to conducting polymer with metal nanoparticle, which not only help in the catalytic oxidation of DA, but also repel AA from the close proximity. In this paper, we report an emulsion polymerization route without using any surfactant for the preparation of PANA and PANA-Au nanocomposite for their comparative structural, electrochemical, thermal and morphological properties. Furthermore, the resultant nanocomposite is used to fabricate interference-free dopamine sensor.

## 2. Experimental

### 2.1 Materials

Anthranilic acid was obtained from Rolex India Ltd, India. The monomer was used after recrystallization. Ammonium peroxodisulphate, hydrochloric acid and chloroform were obtained from Merck, India. Gold chloride (HAuCl<sub>4</sub>) from SRL, Sisco India Ltd. All other chemicals used were of analytical grade. Double-distilled deionized water was used in all the experiments.

### 2.2 Instruments

The electrochemical characterizations were carried out using electrochemical workstation (model CHI7041C), CH-Instrument Inc., Texas, USA. Differential pulse voltammetry was recorded in a single-compartment three electrode cell with a platinum disk/graphite paste as a working electrode, a platinum plate as an auxiliary electrode and Ag/AgCl as a reference electrode. A  $\lambda$ -25 spectrophotometer of Perkin Elmer, Germany (obtained under DAAD Instrument Grant, Germany), was used for spectral analysis. Atomic force microscope (AFM) images were taken using AFM-STM (model PRO 47, NT-MDT, Russia).

Material was spin-coated over glass substrate through its THF solution and AFM images were taken in semi-contact (tapping) mode. XRD and FT-IR characterizations were carried out with an 18 kW rotating anode Rigaku (Japan) powder X-ray diffractometer and a thermo model 5700 FT-IR, Germany, respectively. Thermogravimetric analysis (TGA) measurements were performed on a NETZSCH, STA 409 PC analyser with a heating rate of 10 °C/min under a flow of N<sub>2</sub>-gas. SEM was carried out at an operating voltage of 15–20 kV using Shimadzu SS-550 Super Scan, Japan.

### 2.3 Synthesis of PANA by emulsion polymerization technique

Polymerization process was carried out in a 25 mL conical flask at room temperature (25 °C). Anthranilic acid monomer was dissolved in 12.5 mL chloroform (100 mM). To this solution, a solution of ammonium persulphate (APS) (400 mM) prepared in 2.5 mL 0.5 N H<sub>2</sub>SO<sub>4</sub> added dropwise with constant stirring. After 15 min, a wine-coloured solution was seen, which further becomes a precipitate within 2 h. The resulting solution was kept at 25 ± 1 °C overnight for complete polymerization. After 24 h, a blackish brown precipitate was collected by centrifugation, followed by washing with 0.5 N H<sub>2</sub>SO<sub>4</sub> and finally with water. Polymer was dried under vacuum and the yield was calculated (~65%) to the weight of the monomer.

### 2.4 Synthesis of PANA-Au nanocomposite by emulsion polymerization technique

Polymerization process was carried out in a 25 mL conical flask at room temperature (25 °C). Anthranilic acid monomer was dissolved in 12.5 mL chloroform (100 mM). To this solution, a solution of gold chloride (10 mM) prepared in 2.5 mL 0.5 N H<sub>2</sub>SO<sub>4</sub> was added dropwise with constant stirring. After 15 min, a brownish precipitate was formed, which later consumed the entire solution within 2 h. The resulting solution was kept at 25 ± 1 °C overnight for complete polymerization. After 24 h, the purple brown precipitate was collected by filtration followed by washing with 0.5 N H<sub>2</sub>SO<sub>4</sub> and finally with water. The polymer formed was dried under vacuum and the yield was calculated (~90%) to the weight of monomer and oxidizing agent weight.

## 3. Results and discussion

Chemical synthesis of PANA is scarcely reported in literature because of the high solubility of the polymer in common solvents. In our previous report, we mentioned about the synthesis method of PANA by using various oxidizing agents (Gupta and Prakash 2010). Degree of

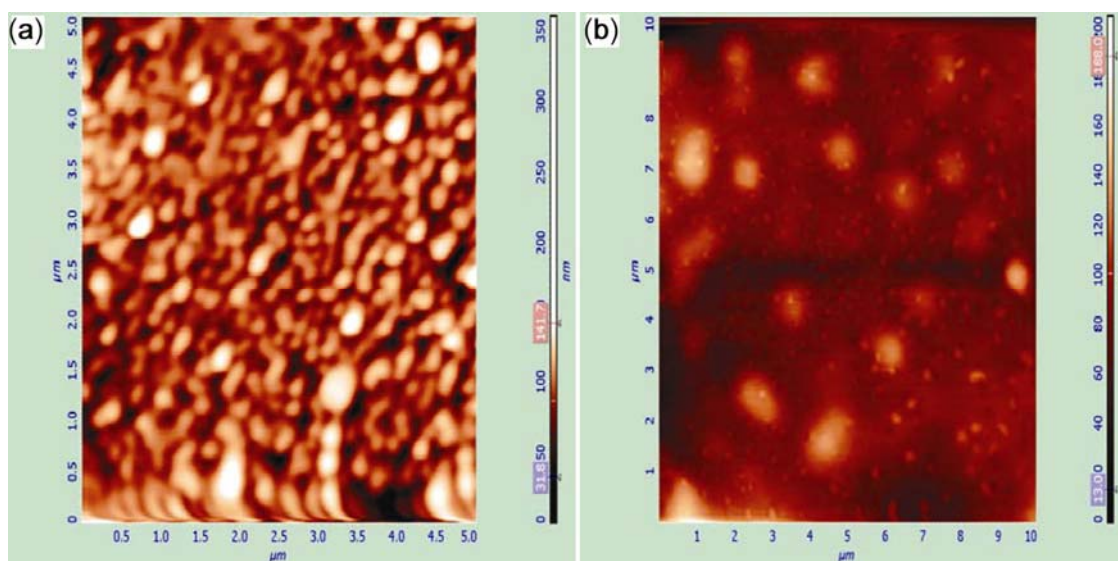


**Figure 1.** AFM images of (a) PANA and (b) PANA–Au nanocomposite.

chain length and various other properties were affected by different types of oxidizing agents. The above synthesis methodology is only limited to the synthesis of pristine polymer. By the use of gold chloride ( $\text{HAuCl}_4$ ) as an oxidizing agent, the polymer formed with the modification is a nanocomposite. We report a simple method to synthesize Au nanoparticles with a reasonable size dispersity using water-soluble conducting polymer colloids of PANA. Mechanism of polymer formation from ions to gold particle ( $\text{Au}^0$ ), which results in the growth, based on the reduction of Au polymer chain simultaneously. Thus, for the growing polymer chain, gold nanoparticles work as a reactive template; over which polymer grows. Au will either form tiny particles or it may collapse into one bigger particle and wrapped by polymeric chain. This depends on various parameters like oxidizing agent concentration, temperature and time of polymerization. Nanocomposite is highly dispersible in non-aqueous solvent that can be used for thin film formation. AFM image of a thin film polymer shows uniform polymeric globules and the nanocomposite depicting the presence of tiny nanoparticles in the polymeric matrix, as shown in figure 1, with average surface roughness of 200 and 114 nm, respectively. SEM images also support the presence of superficial Au nanoparticles. Morphology of polymeric globules is not very uniform in the case of nanocomposites opposite to that of pure polymer, probably because of the strong oxidizing nature of  $\text{HAuCl}_4$  than that of  $(\text{NH}_4)_2\text{S}_2\text{O}_8$ , as shown in figure 2. PANA–Au nanocomposite synthesized by emulsion polymerization route was studied for the reaction kinetics by UV–Vis spectroscopic method with various time intervals of polymerization. UV–Vis spectra of reaction medium were taken for various time interval, viz. 0, 15, 30 min, 1, 2 and 24 h. In the case of emulsion polymerization with  $\text{HAuCl}_4$ , a gradual

fall in  $\text{HAuCl}_4$  absorbance was observed, as shown in figure 3. Complete disappearance of the  $\text{HAuCl}_4$  absorbance was observed after 30 min. Furthermore, the growth of the polymer in case of nanocomposite was observed from the same technique and the resulted spectra are shown in figure 3 (inset). After complete disappearance of  $\text{HAuCl}_4$  absorbance, a clear feature of oligomeric or shorter-chain polymer was observed. First peak at around 320 nm corresponds to  $\pi$ – $\pi^*$  transition present in case of nanocomposite (290 nm in case of polymer synthesized using ammonium persulphate), which is a clear indication of polymer growth with long conjugation length. A new peak was observed at around 440–455 nm after 30 min, because of surface plasmon resonance of gold nanoparticles that merge with the polaronic transition of the polymer after 1 h of polymerization. Broadening in peaks observed in case of 2 h of polymerization depicts an immobilization of the polymer over gold nanoparticle. With further proceeding of polymerization, the peak shifted to higher wavelength region at 500 nm. This could be because of polaronic transition of polymer (with longer chain length) and plasmonic transition of bigger Au nanoparticles. After completion of polymerization for 24 h, the nanocomposite shows a bathochromic shift for all the transitions relative to that of pure polymer, as shown in figure 4, supporting long conjugation length and interaction between the Au and polymer.

The FT–IR spectra of the PANA and PANA–gold nanocomposites carried out in KBr matrix is shown in figure 5. Features of the band are similar with shifting of the wave number to a lower value for the nanocomposite compared to that of pure polymer. The FT–IR spectra showed a characteristic peak at around  $1686\text{ cm}^{-1}$  (absent in the PANi), which may be attributed to the strong

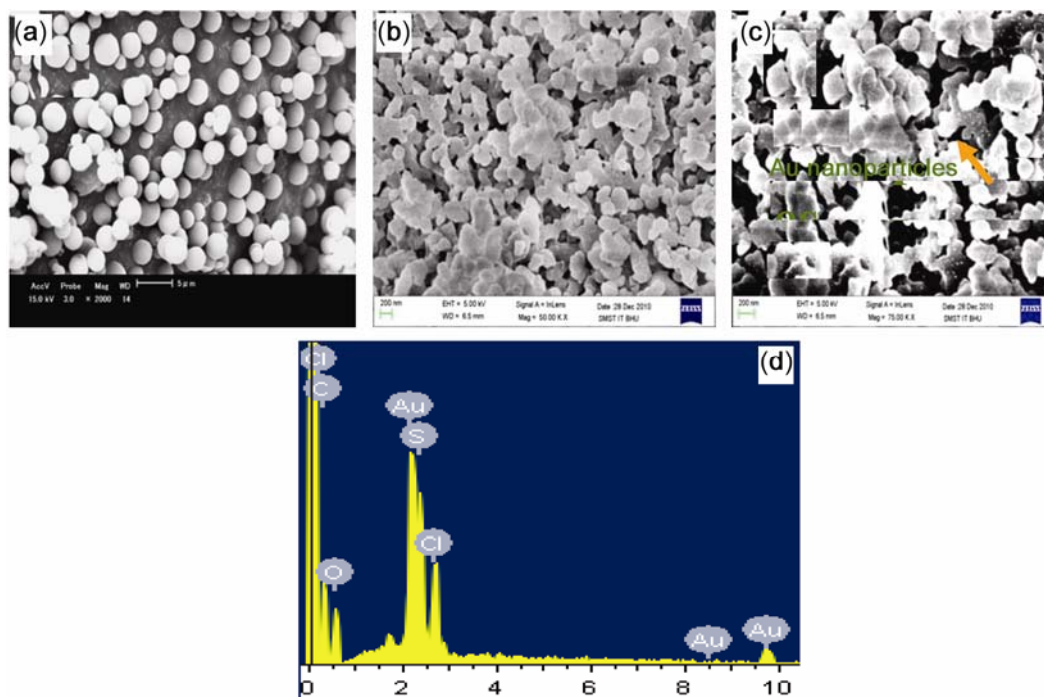


**Figure 2.** SEM images of (a) PANA, (b) PANA–Au nanocomposite, (c) higher magnified PANA–Au nanocomposite showing distributed Au nanoparticles and (d) EDAX data of PANA–Au nanocomposite.

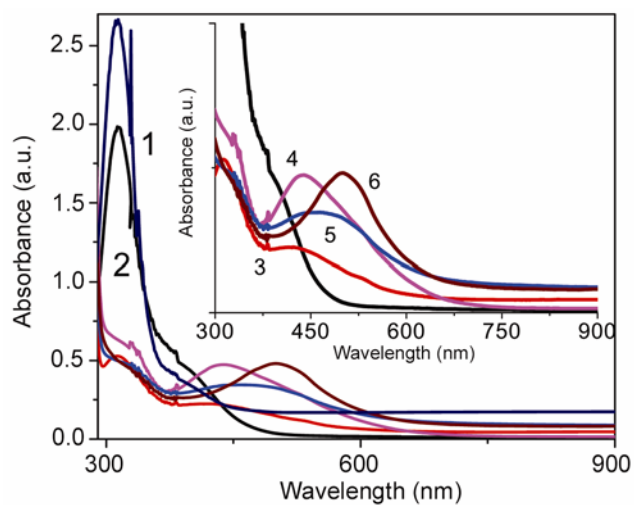


**Figure 3.** UV–Vis of (1) pure gold chloride and (2–6) anthranilic acid– $\text{HAuCl}_4$  reaction mixture after (2) 15 min (3) 30 min (4) 1 h (5) 2 h and (6) 24 h.

stretching vibration of carboxyl group ( $\text{C}=\text{O}$ ) in case of pure polymer synthesized using ammonium persulphate, and shifted to  $1686\text{ cm}^{-1}$  in case of Au nanocomposite. The peak due to  $\text{C}=\text{C}$  bond of benzenoid and quinoid rings are considered for the evaluation of the oxidation states and conjugation in the PANA formed by using ammonium persulphate and gold chloride. The  $\text{C}=\text{C}$  stretching frequency of quinoid and benzenoid rings is observed at  $1563$  and  $1505\text{ cm}^{-1}$  and  $1563$  and  $1508\text{ cm}^{-1}$

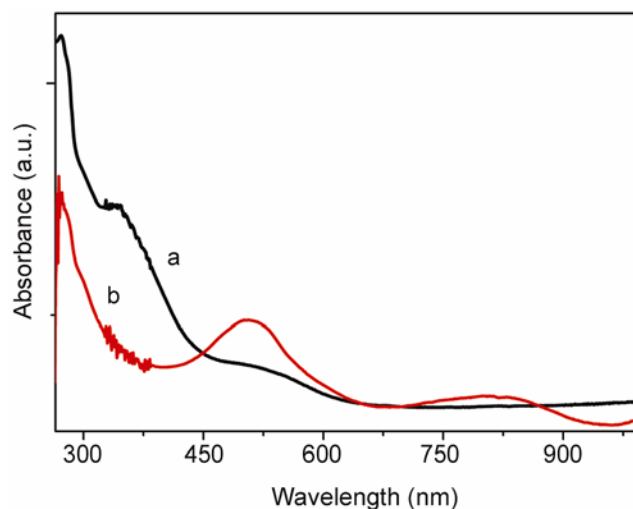


**Figure 4.** UV–Vis spectra of (a) PANA synthesized using  $(\text{NH}_4)_2\text{S}_2\text{O}_8$  and (b) PANA–Au synthesized using  $\text{HAuCl}_4$ .

for the PANA and PANA–Au nanocomposite synthesized using emulsion polymerization route. Intensity ratio ( $I_Q/I_B$ ) of the band is also found to be higher in case of nanocomposite and, hence, supports higher oxidized state of polymer (Reddy *et al* 2008).

Redox property of PANA–Au nanocomposites was studied using differential pulse voltammetric technique. Equal amounts of nanocomposite were coated over platinum disc electrode by spin-casting method through THF

solution. Two pairs of oxidation peaks are observed at 0.28 and 0.55 V, which corresponds to leucomeraldine to emeraldine and emeraldine to pernigraniline transformations (Yue *et al* 1991; Li *et al* 2006) as shown in figure 6(a and b). The peak potential in case of nanocomposite is

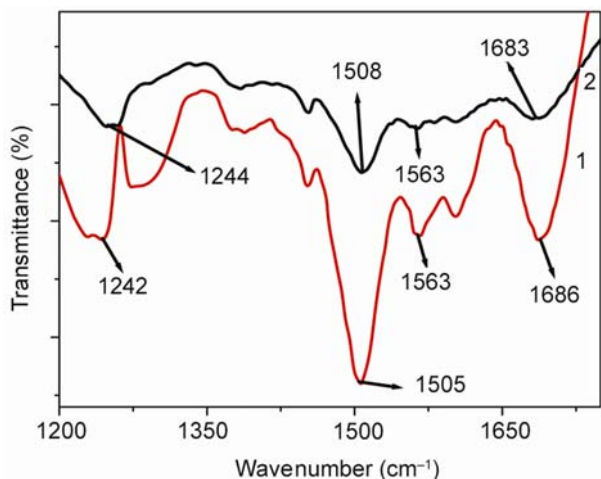


**Figure 5.** FT-IR of (1) PANA synthesized using  $(\text{NH}_4)_2\text{S}_2\text{O}_8$  and (2) PANA–Au synthesized using  $\text{HAuCl}_4$ .

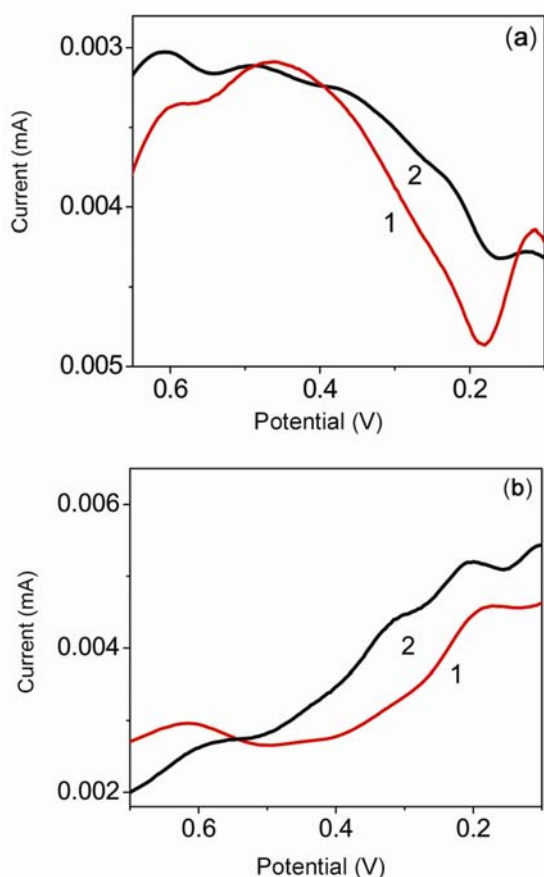


**Figure 6.** Differential pulse voltammery (a) oxidation and (b) reduction of (1) PANA and (2) PANA–Au nanocomposite.

lower than in the case of the pure polymer, probably because of facilitation of these transformations in the presence of Au particles. The relative density of both the transformations depicts a highly oxidized state of the polymer in the presence of Au nanoparticle, which is a clear indication of the charge transfer complex between nanoparticle and polymer. After comparing both the routes, it was found that PANA is more redox active and lesser oxidized than PANA–Au nanocomposite synthesized by emulsion route. This is clearly noticeable by the first redox transformation (not clearly visualized in case of nanocomposite) as shown in figure 6(a).

Formation of gold particles in PANA–Au composite material is highly phase selective as seen in powder XRD pattern (figure 7). A strong (1 1 1) Bragg reflection indicates that gold particles possess a highly oriented crystalline character confirming the face-centred crystal structure (Reddy *et al* 2008). Figure 7 (inset) indicates a less intense and amorphous behaviour of polymer in the

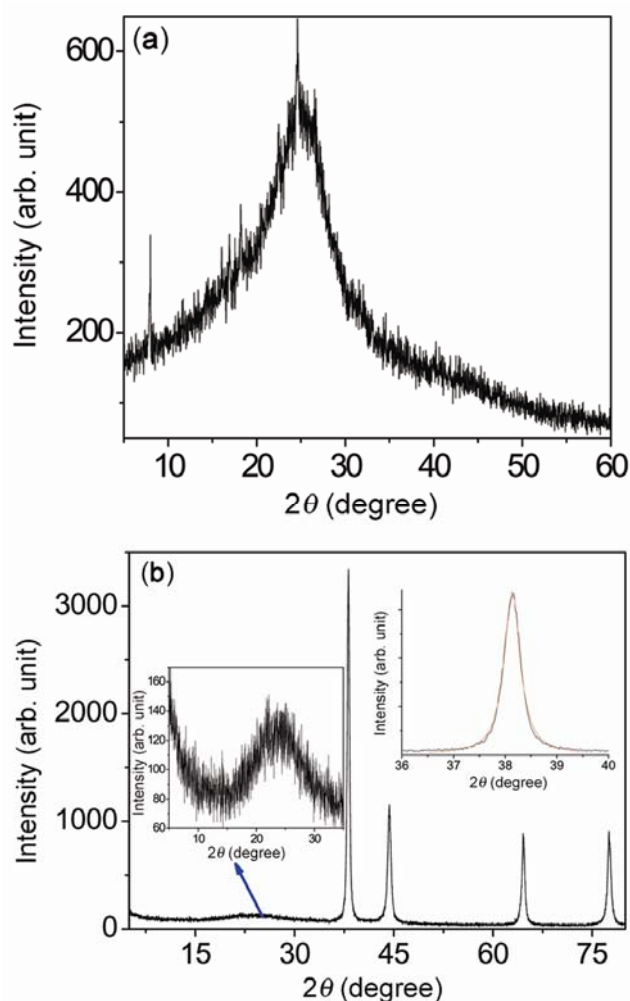


**Figure 7.** XRD pattern of (a) PANA and (b) PANA–Au nanocomposite. Lorentzian best-fit curve for highest intensity peak (inset).

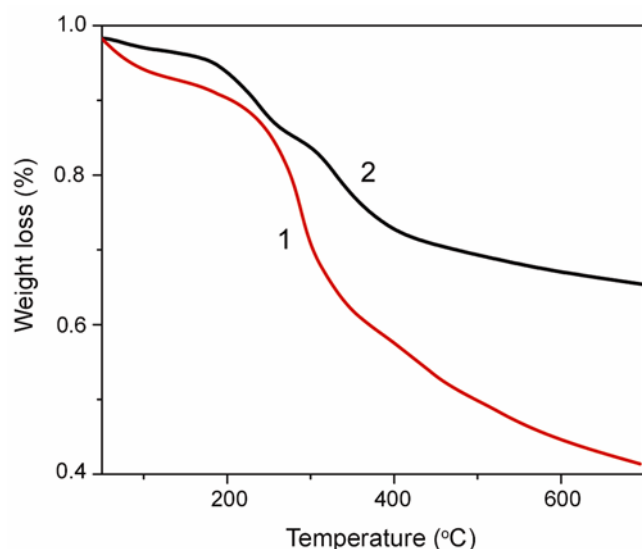
lower  $2\theta$  range from 5 to  $35^\circ$ . Pure polymer shows a comparatively crystalline behaviour with an intense peak at around  $7.8^\circ$  that is because of polymeric self-assembly (Li *et al* 2008). The crystallite size of Au particle can be calculated by line broadening for the highest intense peak using Scherer's equation

$$D = \frac{k\lambda}{\beta \cos \theta} \quad (1)$$

The average size of Au nanoparticles was calculated using (1) and estimated as 24.05 nm for nanocomposites synthesized by emulsion polymerization route. No sharp difference was observed in the diffraction pattern of the polymer.

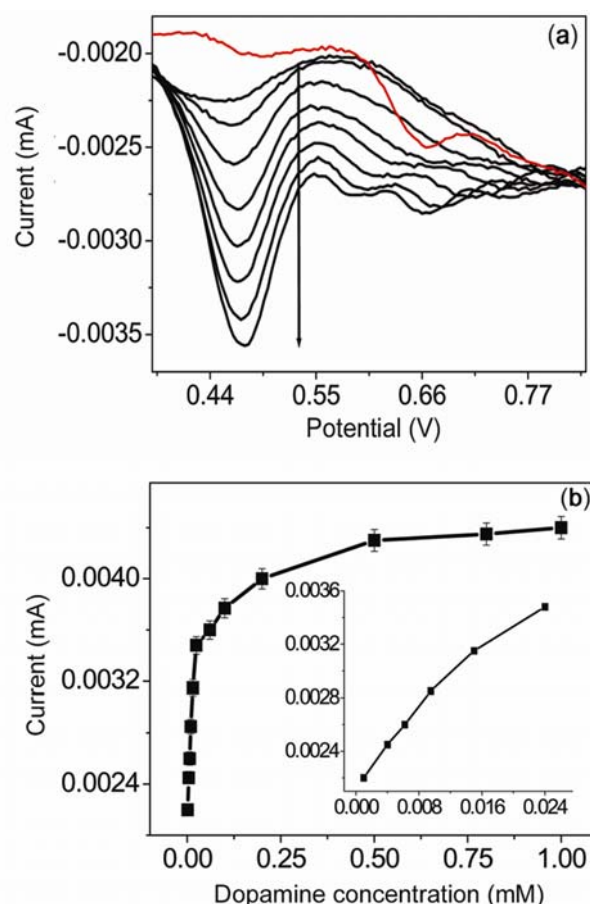
Thermal behaviour of PANA shows a two-step weight loss process (Ogura *et al* 1991) and total weight loss reaches up to 35 and 58% of its original polymer quantity at  $800^\circ\text{C}$  in case of PANA and PANA–Au nanocomposite, respectively as shown in figure 8. The first weight loss at  $180^\circ\text{C}$  in case of pure PANA is attributed to the loss of first pair of carboxylic group. A shift of the same to a higher temperature in case of nanocomposite indicates a higher thermal stability of polymer in presence of Au nanoparticle. The second weight loss starting at around  $300^\circ\text{C}$  in case of PANA–Au nanocomposite is assigned to the loss of second pair of carboxylic group followed by polymer chain degradation ( $410^\circ\text{C}$ ). Two steps of carboxylic group degradation are clearly seen in case of nanocomposite probably because of gradual weight loss; however, in case of pure polymer, second carboxylic group degradation merges with the polymer degradation.

Figure 9(a) depicts the differential pulse voltammograms obtained at graphite paste electrode having 10 wt% of PANA–Au nanocomposite in 10 mM Tris–HCl buffer



**Figure 8.** TGA of (1) PANA and (2) PANA–Au nanocomposite.

(pH 6.8) for different concentrations of DA from  $10^{-6}$  to  $10^{-3}$  M, where the concentration of AA was kept constant (1 mM). It can be observed that almost no response occurs when 1 mM AA was added in the Tris–buffer solution (curve a); this might be because of the acidic group ( $-\text{COOH}$ ) present on the polymer backbone. A sensitivity had been observed for AA on the polymer in the absence of carboxylic functional group. It was also observed that with an increase in DA concentration, oxidation current is also increased (represented by the headed arrow). It is clear that no oxidation peak for AA is present in case of graphite paste electrode modified with PANA–Au. While a broad oxidation peak for DA at 0.46 V was observed, suggesting the selectivity towards DA over modified electrode. The calibration curves for DA detection by DPV at the graphite paste electrode modified with PANA–Au were constructed using average currents recorded at three individual films for each concentration point. Figure 9(b) shows the calibration curves for DA



**Figure 9.** (a) Differential pulse voltammograms of graphite paste electrode modified with PANA–Au with 1 mM AA followed by repeated additions of DA from  $10^{-6}$  to  $10^{-3}$  mM in the presence of 1 mM AA in 10 mM Tris–HCl buffer (pH 6.8). (b) Calibration curve for the analysis of  $10^{-6}$ – $10^{-3}$  M DA over graphite paste modified with PANA–Au (inset: linear part of the curve for sensitivity calculation).

detection in presence of 1 mM AA. The sensitivity towards DA sensing was found to be  $12.5 \mu\text{A} \pm 250 \text{ nA/mM}$ . Further, the lowest detection limit was found to be  $1 \mu\text{M}$ . The enhanced sensitivity, improved linear response and better stability for DA detection without interference further proves its superiority to the earlier work (Mathiyarasu *et al* 2008) related to any conducting polymer–Au modified electrode. The results support the usability of these materials on small-size electrode for getting better sensitivity and selectivity for real-time estimation of DA.

#### 4. Conclusions

Electroactive PANA with spherical morphology and globular PANA–Au nanocomposite was synthesized by two-phase polymerization through emulsion polymerization. Polymer formed by emulsion polymerization was similar to the polymer synthesized by conventional single-phase method, however, showed spherical morphology. Nanocomposite synthesized using  $\text{HAuCl}_4$  having globular morphology with uniformly distributed gold nanoparticles, which reduced the band gap of the polymer and increased thermal property drastically. Nanocomposite of PANA with Au nanoparticles was used for making highly stable, AA interference-free dopamine sensor with sensitivity and lower detection limit of  $12.5 \mu\text{A} \pm 250 \text{ nA/mM}$  and  $10^{-6} \text{ M}$ , respectively. Studies on miniaturized electrode for *in vivo* studies is under progress.

#### Acknowledgement

Authors are thankful to Prof D Panday, SMST, IIT, BHU, for providing XRD facilities and DST, New Delhi, for Inspire Faculty Fellowship.

#### References

- Banik R M, Mayank, Prakash R and Upadhyay S N 2008 *Sens. Actuat. B: Chem.* **131** 295
- Boal K, Ilhan F, DeRouchey J E, Thurn-Albercht T, Russell T P and Rotello V M 2000 *Nature* **404** 746
- Dewald J L, Wondmagegn W T, Ellis A V and Curran S A 2005 *Synth. Met.* **155** 39
- Downard A J, Roddick A D and Bond A M 1995 *Anal. Chim. Acta* **317** 303
- Gupta B and Prakash R 2009 *J. Mater. Sci. Eng.* **C29** 1746
- Gupta B and Prakash R 2010 *Polym. Adv. Technol.* **21** 1
- Hable C T and Wrighton M S 1991 *Langmuir* **9** 1305
- Jin J, Manoharan M P, Wang Q and Haque M A 2009 *Appl. Phys. Lett.* **95** 033113
- Li J, Jia Q, Zhu J and Zheng M 2008 *Polym. Int.* **57** 337
- Li W, Jia Q X and Wang H L 2006 *Polymer* **47** 23
- Maheshwari V and Saraf R F 2006 *Science* **312** 1501
- Majumdar G, Castro E G, Canestraro C D, Zanchet D, Ugarte D, Roman L S and Zarkin A J G 2006 *J. Phys. Chem.* **B110** 17063
- Majumdar G, Goswami M, Sarma M T K, Paul A and Chattopadhyay A 2005 *Langmuir* **21** 1663
- Mallick K, Witcomb M J and Scurrrell M S 2006 *J. Mater. Sci.* **41** 6189
- Mallick K, Witcomb M, Scurrrell M and Strydom A 2009 *J. Phys. D: Appl. Phys.* **42** 095409
- Mathiyarasu J, Senthilkumar S, Phani K L N and Yegnaraman V 2008 *Mater. Lett.* **62** 571
- Melvin A, Vijay R, Chaudhari V R, Gupta B, Prakash R, Haram S, Baskar G and Khushalani D 2010 *J. Coll. Inter. Sci.* **346** 265
- Mirkin C A and Letsinger R L 1996 *Nature* **382** 607
- Mohan S and Prakash R 2010 *J. Mater. Sci. Eng.* **C30** 781
- Nielsen C B and Bjørnholm T 2005 *Macromolecules* **38** 10379
- Ogura K, Shiigi H, Nakayama M and Ogawa A 1999 *J. Polym. Sci. Part A: Polym. Chem.* **37** 4458
- Pandey P C, Chauhan D S and Singh V 2009 *Electrochim. Acta* **54** 2266
- Power A C, Betts A J and Cassidy J F 2010 *Analyst* **13** 1645
- Reddy K R, Lee K P, Lee Y and Gopalan A I 2008 *Mat. Lett.* **62** 1815
- Selvaraj V and Alagar M 2008 *Nanotechnology* **19** 045504
- Singh A K, Joshi L, Prakash R and Kaneto K 2010 *Japanese J. Appl. Phys.* **49** 01AD06
- Singh A K, Prakash R, Dwivedi A D D and Chakrabarti P 2008 *Synth. Metals* **158** 939
- Tseng R J, Huang J, Ouyang J, Richard B, Kaner R B and Yang Y 2005 *Nano Lett.* **5** 1077
- Tu X, Xie Q, Jiang S and Yao S 2007 *Biosens. Bioelectron.* **22** 2819
- Yue J, Wang Z H, Cromack K R, Epstein A J and MacDiarmid A G 1991 *J. Am. Chem. Soc.* **113** 2665